Geophys. J. Int. (2003) **152,** 228–236

An analytical solution for correcting palaeomagnetic inclination error

Xiaodong Tan* and Kenneth P. Kodama

Department of Earth and Environmental Sciences, Lehigh University, Bethlehem, PA 18015, *USA. E-mail: tan@ipgp.jussieu.fr*

Accepted 2002 August 6. Received 2002 July 22; in original form 2002 March 21

SUMMARY

With increasing evidence showing significant inclination shallowing in red beds, it is important to develop useful tools to detecting and correcting inclination errors for haematite-bearing sedimentary rocks. Theoretically, any deviation of magnetization from the ambient magnetic field can be described by a preferred orientation distribution (OD) of unique axes of the anisotropic magnetic particles. Based on Stephenson's continuous particle OD function, magnetic anisotropy parameters of a bulk sample and inclination-correction equations were derived considering all the magnetic particles in a sample. In addition to our new equations for correcting red bed inclination error, the results also confirm the inclination correction of Jackson *et al.* for magnetite-bearing samples, which is based on a simple, discrete-particle OD model used by Stephenson *et al.* to show their derivations, suggesting that the inclination correction is probably independent of the particle OD models.

Key words: inclination error, magnetic anisotropy, palaeomagnetism.

1 INTRODUCTION

Significant inclination shallowing (>15°) of haematite-bearing sediments has been observed in laboratory redeposition experiments (Lovlie & Torsvik 1984; Tauxe & Kent 1984; Tan *et al.* 2002a), in compaction experiments (Tan *et al.* 2002a), and in modern fluvial haematite-bearing deposits (Tauxe & Kent 1984; Rosler & Appel 1998). It has also been observed in the Neogene Siwalik Formation red beds deposited in the Himalayan foreland fluvial and alluvial environments (e.g. Butler 1992; Gautam & Fujiwara 2000; Ojha *et al.* 2000), in Miocene red beds from the extensional Catalan Neogene basins of Spain (Garces *et al.* 1996), in Tertiary and Cretaceous red beds from central Asia (especially, NW China) (e.g. Gilder *et al.* 1996, 2001; Fang *et al.* 1997; Kodama & Tan 1997; Tan *et al.* 2002b), and in Palaeozoic red beds from North America (e.g. van der Pluijm *et al.* 1993; Potts *et al.* 1994; Stamatakos *et al.* 1995; Tan & Kodama 2002). Red beds are one of the major targets of palaeomagnetic studies aimed at constructing major continental apparent polar wander paths and delineating the kinematic histories of major and minor continental blocks. Therefore, it is of great interest to develop useful approaches to detecting and correcting inclination errors in red beds.

Deviation of the magnetization of a sample from the applied magnetic field direction can be theoretically described by an anisotropy in the ability of the sample being magnetized (either by magnetic susceptibility, k_χ, or remanence susceptibility, q_χ) assuming there are no magnetic interactions between magnetic particles. The anisotropy of magnetic susceptibility (AMS) and remanence susceptibility (ARS) of a bulk sample results from an anisotropic orientation distribution (OD) of the anisotropic individual particles. ARS may include the anisotropies of anhysteretic remanence (ARM), isothermal remanence (IRM) and thermal remanence (TRM). Stephenson *et al.* (1986) have derived mathematical relationships between the individual particle anisotropy and bulk sample anisotropy parameters. To avoid mathematical complexities, they used a simple particle OD model in which the magnetically prolate particles are aligned with their maximum anisotropy axes parallel to each of the three principal axes of the bulk sample anisotropy ellipsoid. They stated that the results are the same as if the mathematical relationships are derived using a more realistic, continuous particle OD function, i.e. that proposed by Stephenson (1981). Jackson *et al.* (1991) developed a quantitative model for correcting inclination shallowing carried by magnetite-bearing samples by assuming that the remanence-acquisition tensor of sediments is consistent with the long-axis OD model. In both of these derivations, only those particles with easy axes aligned parallel to the principal axes of the bulk sample anisotropy ellipsoids were considered. Since the contributions of magnetic susceptibility or remanent magnetization from particles not aligned with their easy axes parallel to the three principal axes do not cancel out, this simplification is not sound physically. The anisotropy of haematite particles is most probably oblate, different from the prolate magnetite anisotropy. Therefore, the equation of Jackson *et al.* (1991) is not applicable for haematite-bearing samples. We will use a continuous particle OD function to derive a complete relationship between individual particle anisotropy and bulk sample anisotropy parameters for magnetite-bearing and haematite-bearing samples, respectively, and, in particular, to develop new formulae to detect and correct red bed inclination errors.

*Present address: Institut de Physique du Globe de Paris, Laboratoire de Paleomagnetisme 4, place Jussieu-Tour 24, 75252 Paris cedex 05, France.

2 ASSUMPTIONS

The AMS and ARS of bulk rock samples and their influence on the fidelity of the palaeomagnetic record to the magnetic field direction can be understood based on three essential assumptions concerning the magnetic anisotropy of the individual magnetic particles and the particle OD pattern. First, the magnetic interaction between individual particles is negligible. If this assumption does not hold, the situation is more complicated, and it will not be considered in this study. Secondly, the magnetic anisotropy of individual particles can be expressed by an ellipsoid of revolution. This means that the individual particle anisotropy is either prolate with equal susceptibility in the minimum plane or oblate with isotropic susceptibility in the maximum plane. It can be expressed as

$k_1 > k_2 = k_3$ for prolate particle AMS fabric, $k_1 = k_2 > k_3$ for oblate particle AMS fabric, and

$q_1 > q_2 = q_3$ for prolate particle ARS fabric, $q_1 = q_2 > q_3$ for oblate particle ARS fabric,

where k_i, q_i $(i = 1, 2, 3)$ are the principal axes of the AMS and ARS ellipsoids of the individual particle, respectively.

Then, the individual particle anisotropy factor, a is defined as

$a_\chi = k_1/k_2$ (or k_2/k_3) for magnetic susceptibility of prolate (or oblate) particles, and

$a_\gamma = q_1/q_2$ (or q_2/q_3) for remanence susceptibility of prolate (or oblate) particles.

The third assumption is that the intrinsic (individual particle) remanent magnetization is along the easy axis for prolate particles and within the easy plane for oblate particles. Specifically, the natural remanent magnetization (NRM) of a sample is the vector sum, exclusively, of the magnetizations along the easy axes of individual magnetite particles or the magnetizations within the easy planes of haematite particles. In reality, the latter two assumptions can be met by single-domain or elongated pseudo-single-domain magnetite particles and rhombohedral and hexagonal haematite crystal particles because the easy magnetization axis of a magnetite mineral is controlled by particle shape and a haematite mineral is controlled by magnetocrystalline anisotropy (e.g. Dunlop & Ozdemir 1997). The magnetic susceptibility of haematite is ~ 6000 μSI (e.g. Borradaile & Henry 1997). The magnetic susceptibility of common red beds is <300 μSI. Therefore, the concentration of haematite in red beds is probably <5 per cent. Magnetic interaction between particles is in many cases negligible because of the relatively low concentration of magnetic minerals, except for chemically precipitated magnetic minerals. Magnetic interaction is important between precipitates of magnetite or haematite particles that carry a chemical remanent magnetization (CRM). CRM carried by multiple generations of haematite particles may be parallel or antiparallel to the applied field direction, or without any relation to the field direction (Stokking & Tauxe 1990), suggesting that magnetic interaction of chemical precipitates of haematite can exist. On the other hand, if a complicated remanent magnetization is not observed in real red beds, which is probably a common situation, magnetic interaction is probably not important. Therefore, the three assumptions for inclination-shallowing correction of red beds are generally met.

3 CONTRIBUTION OF A SINGLE PARTICLE

The existence of anisotropic particles is essential, while a preferential OD of anisotropic particles is necessary to cause a deflection

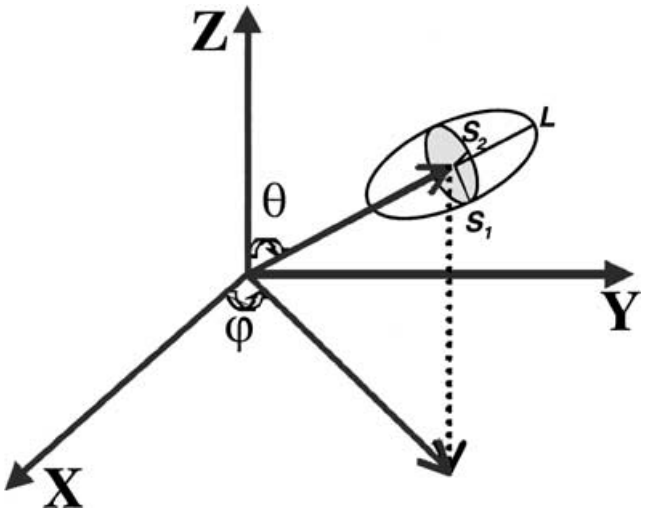

Figure 1. A diagram showing the orientation of a prolate particle in the spherical polar coordinates. The principal axes (**L** and $\mathbf{S}_1$) of the particle anisotropy can be defined by their declination and inclination, i.e. $\mathbf{L}(\varphi, 90^\circ - \theta)$, $\mathbf{S}_1(\varphi, \theta)$, and $\mathbf{S}_2$ is the cross-product of **L** and $\mathbf{S}_1$, which is parallel to the horizontal plane (X–Y).

of the remanent magnetization from the magnetic field direction. A uniform OD of anisotropic particles will not cause a bulk sample anisotropy or inclination error for the sample. Stephenson (1981) derived a particle OD function from the inversion of an anisotropy expression for bulk rock samples; therefore, it was assumed to be a realistic OD function for the anisotropic particles in a sample (Stephenson *et al.* 1986). Derivation of the analytical solution is based on Stephenson's OD function:

$$n(\theta, \varphi) = \frac{3\,N_0}{2\pi}\left[k_z + (k_y - k_z)\sin^2\theta + (k_x - k_y)\sin^2\theta\cos^2\varphi\right], \tag{1}$$

where $n(\theta, \varphi)$ is the angular number density of particles with their unique principal axes of the individual particle aligned in and around the direction defined by unit spherical polar coordinates (θ, φ) (Fig. 1); N_0 is the total number of particles in the distribution; k_x, k_y, k_z are the number densities of particles with their unique principal axes of the individual particle aligned in the three principal axes X, Y and Z of the bulk sample anisotropy ellipsoid divided by $3N_0/2\pi$, respectively. k_x, k_y and k_z have been normalized such that $k_x + k_y + k_z = 1$. The unique principal axis of the individual particle is either the easy axis of a prolate magnetite particle or the hard axis of an oblate haematite particle.

Assuming that the susceptibility values of the unique principal axis of the individual particle and the equal axes are L and S, respectively, the eigenvalues of the anisotropy tensor of the particle are

$$D = \begin{vmatrix} L & & \\ & S & \\ & & S \end{vmatrix}. \tag{2}$$

The anisotropy tensor of a particle aligned in the direction defined by (θ, φ) shown in Fig. 1 is

$$T = PDP^{\mathrm{t}}, \tag{3}$$

where **P** is the eigenvector (unit vectors along L and Ss) matrix of the anisotropy of the particle, and $\mathbf{P}^{\mathrm{t}}$ is the transposed matrix of **P**:

$$P = |\mathbf{A}, \mathbf{B}, \mathbf{C}| = \begin{vmatrix} \sin(\theta)\cos(\varphi) & -\sin(\varphi) & -\cos(\theta)\cos(\varphi) \\ \sin(\theta)\sin(\varphi) & \cos(\varphi) & -\cos(\theta)\sin(\varphi) \\ \cos(\theta) & 0 & \sin(\theta) \end{vmatrix}. \tag{4}$$

By extension of eq. (3), it can be shown that the contributions of either magnetic susceptibility or remanence from a single particle with its unique axis aligned in the direction defined by (θ, φ) to the principal axes, X, Y, Z, of the anisotropy ellipsoid of the bulk sample are T_{11}, T_{22}, T_{33}, respectively:

$$\begin{aligned} T_{11} &= S + (L - S)\cos^2\varphi \sin^2\theta, \\ T_{22} &= S + (L - S)\sin^2\varphi \sin^2\theta, \\ T_{33} &= S + (L - S)\cos^2\theta. \end{aligned} \tag{5}$$

4 BULK SAMPLE ANISOTROPY

Integrating the contributions from all the particles in a sample to the X, Y and Z directions, respectively, one will obtain the bulk sample susceptibility or remanence along the three principal axes of an anisotropy ellipsoid:

$$\begin{aligned} X &= \int_0^{2\pi}\int_0^{\pi/2} T_{11} n(\theta, \varphi)\sin(\theta)\, d\theta\, d\varphi, \\ Y &= \int_0^{2\pi}\int_0^{\pi/2} T_{22} n(\theta, \varphi)\sin(\theta)\, d\theta\, d\varphi, \\ Z &= \int_0^{2\pi}\int_0^{\pi/2} T_{33} n(\theta, \varphi)\sin(\theta)\, d\theta\, d\varphi. \end{aligned} \tag{6}$$

The results of the integration in eq. (6) are:

$$\begin{aligned} X &= (N_0/5)[(L + 4S) + 2(L - S)k_x], \\ Y &= (N_0/5)[(L + 4S) + 2(L - S)k_y], \\ Z &= (N_0/5)[(L + 4S) + 2(L - S)k_z]. \end{aligned} \tag{7}$$

Normalization of X, Y and Z by $(X + Y + Z)$ yields the final normalized principal axes for the bulk sample:

$$\begin{aligned} X_0 &= \frac{2(L - S)k_x + (L + 4S)}{5(L + 2S)}, \\ Y_0 &= \frac{2(L - S)k_y + (L + 4S)}{5(L + 2S)}, \\ Z_0 &= \frac{2(L - S)k_z + (L + 4S)}{5(L + 2S)}. \end{aligned} \tag{8}$$

By solving eq. (8), the three constants, k_x, k_y and k_z, can be expressed as functions of the three measurable parameters X_0, Y_0 and Z_0:

$$\begin{aligned} k_x &= \frac{5(L + 2S)X_0 - (L + 4S)}{2(L - S)}, \\ k_y &= \frac{5(L + 2S)Y_0 - (L + 4S)}{2(L - S)}, \\ k_z &= \frac{5(L + 2S)Z_0 - (L + 4S)}{2(L - S)}. \end{aligned} \tag{9}$$

For elongated magnetite-bearing samples, the a factor is defined by L/S, and eqs (8) and (9) become

$$\begin{aligned} X_0 &= \frac{2(a - 1)k_x + (a + 4)}{5(a + 2)}, \\ Y_0 &= \frac{2(a - 1)k_y + (a + 4)}{5(a + 2)}, \\ Z_0 &= \frac{2(a - 1)k_z + (a + 4)}{5(a + 2)} \end{aligned} \tag{10}$$

and

$$\begin{aligned} k_x &= \frac{5(a + 2)X_0 - (a + 4)}{2(a - 1)}, \\ k_y &= \frac{5(a + 2)Y_0 - (a + 4)}{2(a - 1)}, \\ k_z &= \frac{5(a + 2)Z_0 - (a + 4)}{2(a - 1)}. \end{aligned} \tag{11}$$

Eqs (10) and (11) are different from those used by Stephenson *et al.* (1986). For example, the difference between k_x and k'_x of Stephenson *et al.* (1986) (eq. 5) is $(a + 2)(3X_0 - 1)/[2(a - 1)]$. Furthermore, similar equations are derived for haematite-bearing samples. For flaky oblate haematite particles, the a factor is defined by S/L, and eqs (8) and (9) become

$$\begin{aligned} X_0 &= \frac{2(1 - a)k_x + (1 + 4a)}{5(1 + 2a)}, \\ Y_0 &= \frac{2(1 - a)k_y + (1 + 4a)}{5(1 + 2a)}, \\ Z_0 &= \frac{2(1 - a)k_z + (1 + 4a)}{5(1 + 2a)} \end{aligned} \tag{12}$$

and

$$\begin{aligned} k_x &= \frac{5(1 + 2a)X_0 - (1 + 4a)}{2(1 - a)}, \\ k_y &= \frac{5(1 + 2a)Y_0 - (1 + 4a)}{2(1 - a)}, \\ k_z &= \frac{5(1 + 2a)Z_0 - (1 + 4a)}{2(1 - a)}. \end{aligned} \tag{13}$$

5 INCLINATION CORRECTIONS

Assuming a is infinite for the intrinsic remanent magnetization of individual particles that contribute to the NRM, a tensor for the acquisition of NRM can be derived from eq. (10) for magnetite-bearing samples and from eq. (12) for haematite-bearing samples, respectively:

$$\begin{aligned} k_{\mathrm{NRM}} &= \begin{pmatrix} X_0 & 0 & 0 \\ 0 & Y_0 & 0 \\ 0 & 0 & Z_0 \end{pmatrix} \\ &= \frac{1}{5}\begin{pmatrix} 2k_x + 1 & 0 & 0 \\ 0 & 2k_y + 1 & 0 \\ 0 & 0 & 2k_z + 1 \end{pmatrix} \quad (\mathrm{Fe_3O_4}) \end{aligned} \tag{14}$$

$$k_{\mathrm{NRM}} = \frac{1}{5}\begin{pmatrix} 2 - k_x & 0 & 0 \\ 0 & 2 - k_y & 0 \\ 0 & 0 & 2 - k_z \end{pmatrix} \quad (\alpha\text{-}\mathrm{Fe_2O_3}). \tag{15}$$

The relationship between remanent components [$\mathbf{M}_r = (N_r, E_r, V_r)^t$] and palaeomagnetic field components [$\mathbf{H}_f = (N_f, E_f, V_f)^t$] can be expressed as

$$M_r = k_{NRM} H_f. \tag{16}$$

Assuming the palaeomagnetic field is within the *XZ* plane of the anisotropy ellipsoid, or the anisotropy ellipsoid is oblate with almost equal magnitudes for the maximum and intermediate axes, the remanent inclination of magnetite-bearing samples can be derived from eqs (14) and (16):

$$\tan(I_0) = \frac{2k_x + 1}{2k_z + 1} \tan(I_m). \tag{17}$$

The two constants k_x and k_z can be replaced by bulk sample anisotropy and individual particle anisotropy parameters, eq. (11), using either ARS or AMS measurement results. Inserting eq. (11) into eq. (17), we then have the inclination-correction equation for magnetite-bearing samples:

$$\tan(I_0) = \frac{(a+2)X_0 - 1}{(a+2)Z_0 - 1} \tan(I_m), \tag{18}$$

where I_0 is the real magnetic field inclination; I_m is the remanent inclination; X_0 and Z_0 are the normalized principal anisotropy axes of the bulk rock samples and a is the individual particle anisotropy factor. Eq. (18) is the same as that derived by Jackson *et al.* (1991).

Similarly, the remanent inclination of haematite-bearing samples can be derived from eqs (15) and (16):

$$\tan(I_0) = \frac{2 - k_x}{2 - k_z} \tan(I_m). \tag{19}$$

Inserting eq. (13) into eq. (19), we then have the inclination correction equation for haematite samples:

$$\tan(I_0) = \frac{(2a+1)X_0 - 1}{(2a+1)Z_0 - 1} \tan(I_m). \tag{20}$$

A correction for inclination error may use either the AMS or ARS parameters for bulk samples and individual particles. Measurement of the individual particle anisotropy is difficult, although it is not impossible. Approaches for determining the a factor include compaction experiments and extraction of magnetite particles (e.g. Kodama 1997; Tan & Kodama 1998). Laboratory compaction experiments of disaggregated sediments may provide a more accurate estimate of the a factor, yet disaggregation and compaction experiments are not easily applied to well-cemented and/or coarse-grained sediments. Direct measurement of the a factor involves disaggregation of sediments, extraction of magnetic particles and alignment of the easy axes of the particles parallel to a magnetic field. This approach is less accurate and more difficult, because extracting only those particles that carry the characteristic remanent magnetization (ChRM) is difficult, and magnetic interaction between the extracted particles is almost inevitable. Separation of fine haematite particles from red beds is even more difficult. Alternatively, Stephenson *et al.* (1986) suggested that the a factor may be constrained using the relationship between the normalized bulk sample AMS and the ARS principal axis values (χ_i, R_i).

6 RELATIONSHIPS BETWEEN AMS AND ARS

Rewrite eq. (11) for magnetic susceptibility and remanence, respectively; by equating these two equations (because of the same particle distribution) and rearranging, we then have a relationship between normalized AMS and ARS principal axes for magnetite-bearing samples:

$$R_i = \frac{(a_\chi + 2)(a_\gamma - 1)}{(a_\gamma + 2)(a_\chi - 1)} \chi_i + \frac{a_\chi - a_\gamma}{(a_\gamma + 2)(a_\chi - 1)}, \tag{21}$$

where a_χ and a_γ are the magnetic susceptibility and remanence anisotropy factors of the individual particle, respectively; $R_i = R_1$, R_2, R_3, are the normalized ($R_1 + R_2 + R_3 = 1$) maximum, intermediate and minimum axes of ARS, and $\chi_i = \chi_1$, χ_2, χ_3, are the normalized ($\chi_1 + \chi_2 + \chi_3 = 1$) maximum, intermediate and minimum axes of AMS.

We find a similar relationship for haematite-bearing samples:

$$R_i = \frac{(2a_\chi + 1)(a_\gamma - 1)}{(2a_\gamma + 1)(a_\chi - 1)} \chi_i + \frac{a_\chi - a_\gamma}{(2a_\gamma + 1)(a_\chi - 1)}. \tag{22}$$

Following Stephenson *et al.* (1986), by defining the normalized particle a factor as

$$\bar{a}_\gamma = \frac{a_\gamma}{2 + a_\gamma}, \quad \bar{a}_\chi = \frac{a_\chi}{2 + a_\chi} \quad (\text{for } Fe_3O_4) \tag{23}$$

$$\bar{a}_\gamma = \frac{a_\gamma}{1 + 2a_\gamma}, \quad \bar{a}_\chi = \frac{a_\chi}{1 + 2a_\chi} \quad (\text{for } \alpha\text{-}Fe_2O_3) \tag{24}$$

it can be shown that the normalized a factors for remanence and magnetic susceptibility have the same linear relationship as eq. (21) for magnetite or eq. (22) for haematite. Although the values of the normalized a factors are between 1/3 and 1 for magnetite particles, and between 1/3 and 1/2 for haematite particles, corresponding to the range of the a factor values between 1 and infinity, a much smaller range of either the normalized remanence a factor or the normalized a factor of magnetic susceptibility may be achieved when the slope defined in eq. (21) or (22) is either flat or steep. A few inconsistent data values concerning haematite particle anisotropy have been reported. For example, Neel (1953) measured magnetic susceptibility and saturation remanence as a function of temperature in the direction parallel and perpendicular to the basal plane of the haematite particle, yielding a factor values of less than 1.1 for magnetic susceptibility and approximately 2 for remanence at room temperature. In contrast, Uyeda *et al.* (1963) reported a factor values greater than 100 for magnetic susceptibility. The linear relationship between the remanence and magnetic susceptibility anisotropy-parameters of the bulk sample can be very helpful in determining the a factor of the haematite (e.g. Tan & Kodama 2002; Tan *et al.* 2002b).

The linear relationship between the normalized principal axes of AMS and ARS is for pseudo-single-domain and multidomain magnetite and single-domain and pseudo-single-domain haematite particles. For single domain magnetite particles, the ARS ellipsoid is consistent with the individual particle shape, while the AMS ellipsoid is inverted such that the maximum and minimum axes are along the short and long axes of the particle, respectively (e.g. Potter & Stephenson 1988). The inclination correction equation (eq. 18) may not be applicable for multidomain magnetite, since its intrinsic remanence may not be parallel to the long axis of the particle. In addition, the linear relationship may not apply for bulk rock samples, because AMS measurements often include contributions from ferromagnetic, (super) paramagnetic and diamagnetic particles. Nevertheless, the linear relationship provides an independent way for estimating the a factor value. When ferromagnetic grains dominate the AMS, the easily measured AMS and ARS parameters may be analysed by linear regression. The values of the slope and the intercept point on the R_i axis (eqs 21 or 22), can be used to constrain the a factors of the individual particles in the bulk samples.

When the *a* factor is known, an accurate palaeomagnetic inclination can be determined by eq. (18) for magnetite-bearing or eq. (20) for haematite-bearing samples, respectively.

7 DISCUSSION

Jackson *et al.* (1991) derived an inclination-correction expression for magnetite-bearing samples, which is the same as eq. (18). They used the simple relationship between remanence anisotropy and individual particle anisotropy of Stephenson *et al.* (1986) and their supposition that the acquisition tensor of the detrital remanent magnetization (DRM) is consistent with the long-axis OD function:

$$k_D = \begin{pmatrix} k_D\,\max & 0 & 0 \\ 0 & k_D\,\mathrm{int} & 0 \\ 0 & 0 & k_D\,\min \end{pmatrix} = \begin{pmatrix} k_x & 0 & 0 \\ 0 & k_y & 0 \\ 0 & 0 & k_z \end{pmatrix}. \qquad (25)$$

The basic assumptions we used are essentially the same as those implicit in their derivations, but we consider the contributions from all the magnetic particles. Eqs (20) and (22) can be derived following their reasoning. However, by considering all magnetic particles, we have derived new relationships between individual particle and bulk sample anisotropies (eqs 8–15), which indicate that the contribution of individual particles not aligned with their ellipsoid axes parallel to the principal axes of the bulk sample cannot be neglected. If these new relationships are used in the DRM tensor of Jackson *et al.* (1991) (eq. 25), we will have a different inclination correction equation. For example, the equation for magnetite-bearing samples will be

$$\tan(I_0) = \frac{(a+2)X_0 - (a+4)/5}{(a+2)Z_0 - (a+4)/5}\tan(I_\mathrm{m}). \qquad (26)$$

Eq. (26) yields a significantly greater inclination correction than eq. (18) (Fig. 2). Therefore, Jackson *et al.*'s (1991) DRM tensor is a model-dependent expression for inclination shallowing, which is true for the simplified particle distribution model Stephenson *et al.* (1986) used to show the derivations. In fact, the DRM or NRM tensor depends on detailed OD models. If a truncated Fisher (1953) function (Hrouda 1980) is used as a continuous OD model, it will yield different NRM tensors (see the Appendix). However, eqs (14) and (15) are probably the more realistic tensors of a natural remanent magnetization for magnetite-bearing and haematite-bearing samples, respectively, because they are based on a more realistic OD model (Stephenson 1981).

Three continuous functions have been used to describe OD models, and to derive the relationship between bulk sample anisotropy and individual particle anisotropy. They are the Bingham distribution function (Bingham 1964), the truncated Fisher distribution function (Hrouda 1980) and the Stephenson (1981) distribution function. Both Bingham's and Stephenson's functions describe triaxial OD models, while the Fisher function is a uniaxial OD model. Owens (1974) used numerical approaches to solve the integrations using the Bingham function. We have difficulty in deriving an analytical solution for correcting inclination shallowing using the Bingham function. Stephenson (1981) derived the triaxial OD function by inverting the ellipsoid equation of bulk sample anisotropy; therefore, the function has a physical basis, i.e. the triaxial bulk sample anisotropy. One drawback of the Stephenson (1981) OD model is that it cannot describe the extreme case when particles are perfectly aligned with their unique axis in one direction, because the inversion of the ellipsoid equation for the bulk sample anisotropy does not exist. For the Stephenson OD model, when $k_y = k_z = 0$ and $k_x = 1$ for magnetite-bearing samples or $k_x = k_y = 0$ and $k_z = 1$ for haematite-bearing samples, the model-dependent eqs (10), (17), (12), (19) predict limits for the maximum anisotropy and inclination correction factors, which are 3 and 2 for magnetite-bearing and haematite-bearing samples, respectively. These are the largest anisotropies the model can describe, owing to the small decrease of the OD function near the *Y* and *Z* axes (Fig. 3). Although greater values of anisotropy may occasionally be observed in highly deformed metamorphic rocks, the observed bulk sample anisotropy of sedimentary rocks is well below the limit (e.g. Tarling & Hrouda 1993), suggesting that the Stephenson OD model is valid for studying magnetic anisotropy and inclination corrections of sedimentary rocks. The inclination correction factors calculated using the model-independent eqs (18) and (20) can be greater than these limits (e.g. Fig. 2). This probably indicates that when k_y and k_z (k_x and k_y) are taken as virtual numbers, eqs (10), (12), (17), (19) might predict greater anisotropy and inclination correction factor values. In contrast, the truncated Fisher OD function (Hrouda 1980) can describe the extremely high anisotropies because the OD of particles in the model can be distributed within a very narrow solid angle (Fig. 3). When *k* approaches infinity, $F(k) = -1$, $X_0 = a/(a+2)$, $Y_0 = Z_0 = 1/(a+2)$ and $I_\mathrm{m} = 0^\circ$, eqs (A3), (A5), (A7) (see the Appendix); these parameters are consistent with the extreme model in which the OD is perfectly restricted parallel to the *X*-axis. The truncated Fisher function (Hrouda 1980) can only describe oblate bulk sample ellipsoids if individual particles are oblate, or prolate bulk sample ellipsoids if individual particles are prolate. In contrast, the Stephenson OD function can describe prolate, oblate and triaxial bulk sample anisotropies, independently of whether the anisotropy of the individual particle is prolate or oblate. Choosing the Stephenson OD function in our analytical solution is not only a result of its physical basis but also owing to its ability to describe various anisotropy ellipsoids.

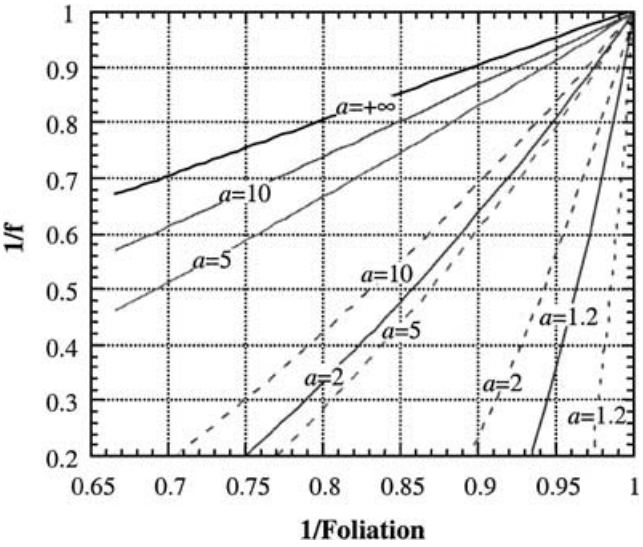

Figure 2. Plots of the inverse of the inclination correction factor ($1/f$) as a function of the inverse of the foliation ($1/F$) of bulk sample anisotropy for certain magnetite particle anisotropy factors, *a*. The solid and dashed lines are calculated by eqs (18) and (26). Eq. (26) is derived by inserting the new relationship (eq. 11) between bulk sample and individual particle anisotropies into the DRM tensor of Jackson *et al.* (1991) (eq. 25). It indicates that the DRM tensor and the NRM tensor are model dependent. However, the relationship between the ARS and AMS principal axes of the bulk sample and the inclination correction expressions are probably model independent (see the text).

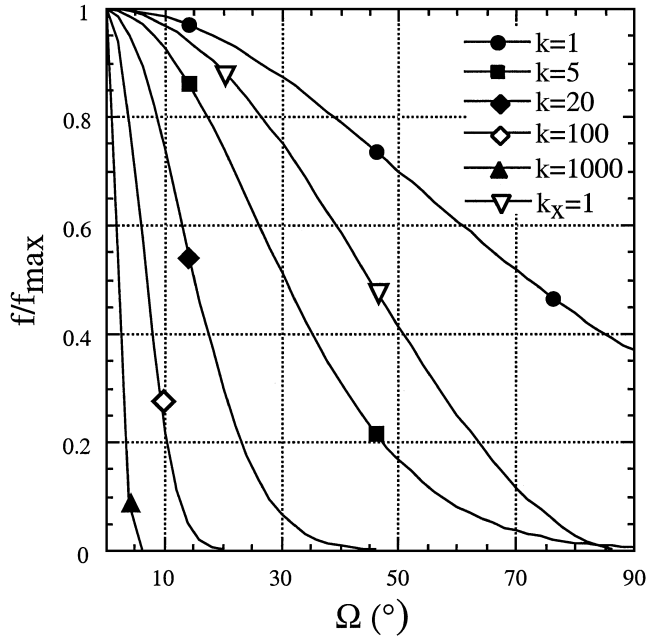

Figure 3. Curves showing the normalized orientation distribution (OD) density of particles with their unique axes aligned in the direction with Ω (=arccos (cos φ ∗ sin θ)) degree to the X-axis. The curves are calculated by the truncated Fisher distribution function (Hrouda 1980) (see the Appendix), $f/f_{\max} = e^{k(\cos\Omega - 1)}$. For comparison, ky and kz are set to zero in Stephenson (1981) OD function, so that the distribution becomes uniaxial, and $f/f_{\max} = \cos^2\Omega$. It shows that the truncated Fisher distribution function is able to describe the extreme cases when OD of particles is restricted in a very narrow solid angle, while the Stephenson's OD model describes a rather smooth OD.

Despite the difference in detailed OD functions, and the model-dependent expressions for the principal axes of bulk sample anisotropy and the remanence tensors, using the truncated Fisher OD function yields the same inclination-correction equations and the same linear relationships between the ARS and AMS principal axes as those derived using the Stephenson OD function and the discrete OD model of Stephenson *et al.* (1986) and Jackson *et al.* (1991) (see the Appendix).

Cogne (1987) derived a theoretical relationship between the ratio of ARS principal axes and the ratio of AMS principal axes for multidomain magnetite, in which the former is the square of the latter, i.e. $P_\gamma = P_\chi^2$. A Peruvian gabbro and granites of Flamanville from NW France yielded exponent values of 1.94 and 1.81, respectively. These results were thought to be in good agreement with the theoretical analysis (Cogne 1987). Recently, Gattacceca & Rochette (2002) observed significantly greater exponent values (3.9) from volcanic flows from Monte Minerva, Italy. The relationship between the degree of ARS and the degree of AMS (defined as the ratio between the maximum and the minimum principal axes) can also be derived from the linear relationship between the ARS and AMS principal axes (eqs 21 or 22):

$$P_\gamma = \frac{sP_\chi + i(1+2P_\chi)}{s + i(1+2P_\chi)} \quad \text{for oblate bulk sample anisotropy} \quad (27)$$

$$P_\gamma = \frac{sP_\chi + i(2+P_\chi)}{s + i(2+P_\chi)} \quad \text{for prolate bulk sample anisotropy} \quad (28)$$

where s and i are the slope and intercept of the line defined by eqs (21) or (22), and $s = 1 - 3i$. P_γ and P_χ do not have a square relationship. The relationship depends on the anisotropy of the individual particle and the bulk sample anisotropy, which can vary quite significantly. The curves derived from real data also deviate significantly from Cogne's theoretical results (Fig. 4), indicating that the square relationship between the degrees of anisotropy of ARS and AMS is probably not universal.

Another critical point for the comparison of ARS and AMS parameters, and for the inclination correction is that the ARS, AMS and ChRM should be carried by the same populations of magnetic particles. Because the highest coercivity of haematite is far greater than 100 mT (the highest alternating field (AF) available to most ARM experiments), the anisotropy of high-field IRM or TRM must be measured to study the anisotropy of remanence-carrying particles and its effect on the palaeomagnetic directions in red beds. When working with AMS, it is important to isolate various sources contributing to AMS. For magnetite-bearing samples, the magnetic susceptibility of bulk samples may be dominated by magnetite. However, when the magnetite is a mixture of single-domain, pseudo-single domain and multidomain particles, separating their contributions to AMS becomes critical. For haematite-bearing samples, owing to its low magnetic susceptibility, it is essential to isolate them from other non-remanence-carrying particles. We have used AF demagnetization to target the anisotropy of ARM of ChRM-carrying magnetite particles (Tan & Kodama 1998), thermal demagnetization to target the anisotropy of IRM of ChRM-carrying haematite particles (Tan & Kodama 2002), and chemical demagnetization to target AMS of ChRM-carrying haematite particles (Tan *et al.* 2002b). Successful inclination corrections rely on a direct relationship between the magnetic anisotropy and the ChRM-carrying particles.

Various processes ranging from syn-depositional, post-depositional to compactional alignment of magnetic particles may have affected the particle distribution pattern. Detailed mechanisms may include interaction between hydraulic, magnetic and mechanical forcing factors during settling of magnetic particles (e.g. Verosub 1977; Tauxe & Kent 1984), attachment of magnetic particles to clay minerals during deposition (Lu *et al.* 1990; Deamer & Kodama 1990) and post-deposition mechanical compaction (Sun & Kodama 1992), and a possible pressure solution (chemical) compaction (Tan & Kodama 2002). Yet, the magnetic anisotropy tensors measured represent the final state of the particle distribution; it may be produced by one or a combination of several mechanisms. The inclination correction developed by Jackson *et al.* (1991) has accurately corrected synthetic magnetite-bearing depositional and compaction-caused inclination shallowing, respectively (e.g. Jackson *et al.* 1991; Kodama & Sun 1992). The new equations developed in this study have also been successfully applied to correct red bed palaeomagnetic inclination shallowing of possible depositional and compactional origins (Tan & Kodama 2002; Tan *et al.* 2002b). Therefore, as suggested by Jackson *et al.* (1991), the inclination correction is not complicated by detailed physical paths of inclination shallowing.

Tectonic strain can also distort the particle distribution pattern and palaeomagnetic directions (e.g. Cogne *et al.* 1986; van der Pluijm 1987; Kodama 1988; Borradaile 1993; Jackson *et al.* 1993). The inclination correction techniques may be applicable to tectonic-strain-deflected remanence. However, since stress and strain may also alter the domain states and magnetic properties of magnetic particles (see, e.g., Jackson *et al.* 1993), the case of strained remanence and magnetic anisotropy is more complicated than the situation we considered here for depositional and burial compaction-caused inclination shallowing. We have not tried to use the techniques developed by Jackson *et al.* (1991) and this study to correct the tectonically distorted palaeomagnetic direction.

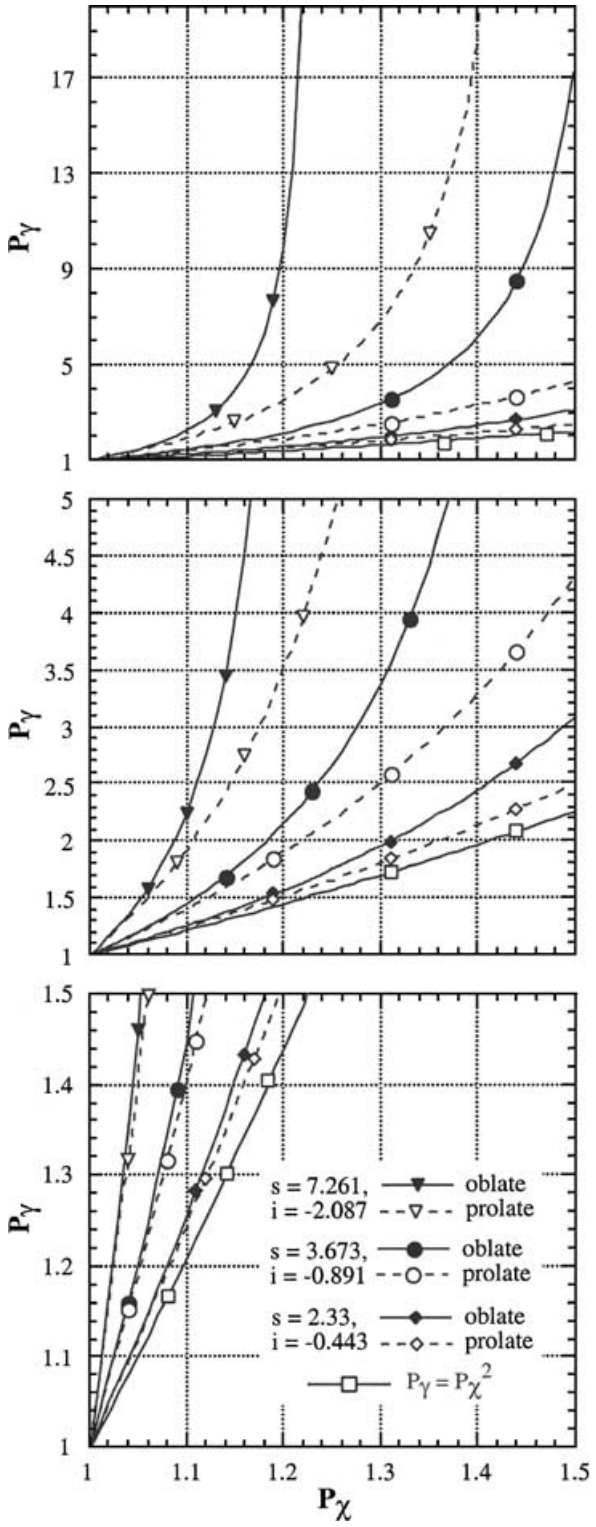

Figure 4. Plots of curves showing the relationship between the degree of ARS and the degree of AMS (eqs 27 and 28). The values of s and i used in the equations are 2.33 and −0.443 of multidomain magnetite-bearing samples from Stephenson *et al.* (1986) Fig. 4 (diamond), 3.673 and −0.891 of haematite-bearing samples from Tan (2001) Fig. 4.16 (circle), 7.261 and −2.087 of haematite-bearing samples from Tan (2001) Fig. 3.19 (triangle). The degree of anisotropy is defined as the ratio between the maximum and minimum principal axes. Note the difference between the magnetite curves (diamond) and the curve defined by the square relationship of Cogne (1987) (square).

8 CONCLUSIONS

Based on three assumptions for individual particle anisotropy, a bulk sample anisotropy is derived from all particles that can be described by a continuous-particle OD function proposed by Stephenson (1981). The expression for a bulk sample anisotropy is different by those derived from only considering particles with their unique axes parallel to the principal axes of the bulk sample, indicating that the other particles also contribute to the bulk sample anisotropy. However, the linear relationship between the ARS and AMS principal axes of the normalized bulk sample and inclination corrections are probably independent of the particle OD models, and independent of detailed mechanisms that may have caused the observed, depositional and/or burial compaction-caused magnetic anisotropy and inclination shallowing.

ACKNOWLEDGMENTS

We are very pleased to acknowledge the kind reply from Dr A. Stephenson to our inquiry concerning his pioneering work. Dr W.H. Owens made critical comments on an earlier version of the manuscript, which together with those of Dr G. Borradaile's helped us to clarify several issues. A very thoughtful and constructive review by Dr M. Jackson led to a fuller discussion and an appendix. This study is supported by NSF grant EAR-9804965 (to KPK).

REFERENCES

Bingham, C., 1964. Distribution on the sphere and on the projective plane, *PhD thesis,* Yale University, New Haven, CT.

Borradaile, G.J., 1993. Deformation and palaeomagnetism, *Surv. Geophys.,* **18**, 405–435.

Borradaile, G.J. & Henry, B., 1997. Tectonic applications of magnetic susceptibility and its anisotropy, *Earth-Sci. Rev.,* **42**, 49–93.

Butler, R.F., 1992. *Palaeomagnetism: Magnetic Domains to Geologic Terranes,* Blackwell, Boston.

Cogne, J.P., 1987. TRM deviations in anisotropic assemblages of multidomain magnetite, *Geophys. J. R. astr. Soc.,* **91**, 1013–1023.

Cogne, J.P., Perroud, H., Trexier, M.P. & Bonhommet, 1986. Strain reorientation of haematite and its bearing upon remanent magnetization, *Tectonics,* **5**, 753–767.

Deamer, G.A. & Kodama, K.P., 1990. Compaction-induced inclination shallowing in synthetic and natural clay-rich sediments, *J. geophys. Res.,* **95**, 4511–4530.

Dunlop, D.J. & Ozdemir, O., 1997. *Rock Magnetism: Fundamentals and Frontiers,* Cambridge University Press, Cambridge.

Fang, D., Tan, X. & Kodama, K.P., 1997. New palaeomagnetic data of Cretaceous and Tertiary red beds from the northern Tarim Basin, northwest China provide more evidence for anomalously shallow inclinations, *EOS, Trans. Am. geophys. Un.,* **78**, Fall Meet. Suppl., F174.

Fisher, R., 1953. Dispersion on a sphere, *Proc. R. Soc. London,* A., **217**, 295–305.

Garces, M., Pares, J.M. & Cabrera, L., 1996. Further evidence for inclination shallowing in red beds, *Geophys. Res. Lett.,* **23**, 2065–2068.

Gattacceca, J. & Rochette, P., 2002. Pseudopalaeosecular variation due to remanence anisotropy in a pyroclastic flow succession, *Geophys. Res. Lett.,* **29**, doi:10.1029/2002GL014 697.

Gautam, P. & Fujiwara, Y., 2000. Magnetic polarity stratigraphy of Siwalik Group sediments of Karnali River section in western Nepal, *Geophys. J. Int.,* **142**, 812–824.

Gilder, S., Zhao, X., Coe, R., Meng, Z., Courtillot, V. & Besse, J., 1996. Palaeomagnetism and tectonics of the southern Tarim basin, northwestern China, *J. geophys. Res.,* **101**, 22 015–22 031.

Gilder, S., Chen, Y. & Sen, S., 2001. Oligo–Miocene magnetostratigraphy and rock magnetism of the Xishugou section, Subei (Gansu Province, western China) and implications for shallow inclinations in central Asia, *J. geophys. Res.,* **106**, 30 505–30 521.

Hrouda, F., 1980. Magnetocrystalline anisotropy of rocks and massive ores: a mathematical model study and its fabric implications, *J. Struc. Geol.,* **2**, 459–462.

Jackson, M.J., Banerjee, S.K., Marvin, J.A., Lu, R. & Gruber, W., 1991. Detrital remanence inclination errors and anhysteretic remanence anisotropy: quantitative model and experimental results, *Geophys. J. Int.,* **104**, 95–103.

Jackson, M., Borradaile, G., Hudleston, P. & Banerjee, S., 1993. Experimental deformation of synthetic magnetite-bearing calcite sandstones: effects on remanence, bulk magnetic properties, and magnetic anisotropy, *J. geophys. Res.,* **98**, 383–401.

Kodama, K.P., 1988. Remanence rotation due to rock strain during folding and the stepwise application of the fold test, *J. geophys. Res.,* **93**, 3357–3371.

Kodama, K.P., 1997. A successful rock magnetic technique for correcting palaeomagnetic inclination shallowing: Case study of the Nacimiento Formation, New Mexico, *J. geophys. Res.,* **102**, 5193–5206.

Kodama, K.P. & Sun, W.W., 1992. Magnetic anisotropy as a correction for compaction-caused palaeomagnetic inclination shallowing, *Geophys. J. Int.,* **111**, 465–469.

Kodama, K.P. & Tan, X., 1997. Central Asian inclination anomalies: possible inclination shallowing in red beds? *Eos Trans.,* **78**, F174.

Lovlie, R. & Torsvik, T., 1984. Magnetic remanence and fabric properties of laboratory deposited haematite-bearing red sandstone, *Geophys. Res. Lett.,* **11**, 229–232.

Lu, R., Banerjee, S.K. & Marvin, J., 1990. The effects of clay mineralogy and the electrical conductivity of water on the acquisition of DRM in sediments, *J. geophys. Res.,* **95**, 4531–4545.

Neel, L., 1953. Some new results on antiferromagnetism and ferromagnetism, *Rev. Mod. Phys.,* **25**, 58–63.

Ojha, T.P., Butler, R.F., Quade, J., Decelles, P.G., Richards, D. & Upreti, B.N., 2000. Magnetic polarity stratigraphy of the Neogene Siwalik Group at Khutia Khola, far western Nepal, *Geol. Soc. Am. Bull.,* **112**, 424–434.

Owens, W.H., 1974. Mathematical model studies on factors affecting the magnetic anisotropy of deformed rocks, *Tectonophysics,* **24**, 115–131.

Potter, D.K. & Stephenson, A., 1988. Single-domain particles in rocks and magnetic fabric analysis, *Geophys. Res. Lett.,* **15**, 1097–1100.

Potts, S.S., van der Pluijm, B.A. & Van der Voo, R., 1994. Discordant Silurian palaeolatitudes for central Newfoundland: new palaeomagnetic evidence from the Springdale Group, *Earth planet. Sci. Lett.,* **120**, 1–12.

Rosler, W. & Appel, E., 1998. Fidelity and time of the magnetostratigraphic record in Siwalik sediments: high-resolution study of a complete polarity transition and evidence for cryptochrons in a Miocene fluviatile section, *Geophys. J. Int.,* **135**, 867–875.

Stamatakos, J., Lessard, A.M., van der Pluijm, B.A. & Van der Voo, R., 1995. Palaeomagnetism and magnetic fabrics from the Springdale and Wigwam red beds of Newfoundland and their implications for the Silurian palaeolatitude controversy, *Earth planet. Sci. Lett.,* **132**, 141–155.

Stephenson, A., 1981. Gyromagnetic remanence and anisotropy in single-domain particles, rocksand magnetic recording tape, *Phil. Mag. B.,* **44**, 635–664.

Stephenson, A., Sadikun, S. & Potter, D.K., 1986. A theoretical and experimental comparison of the anisotropies of magnetic susceptibility and remanence in rocks and minerals, *Geophys. J. R. astr. Soc.,* **84**, 185–200.

Stokking, L.B. & Tauxe, L., 1990. Multicomponent magnetization in synthetic haematite, *Phys. Earth planet. Inter.,* **65**, 109–124.

Sun, W.W. & Kodama, K.P., 1992. Magnetic anisotropy, scanning electron microscopy, and X ray pole figure goniometry study of inclination shallowing in a compacting clay-rich sediment, *J. geophys. Res.,* **97**, 19 599–19 615.

Tan, X. & Kodama, K.P., 1998. Compaction-corrected inclinations from southern California Cretaceous Marine sedimentary rocks indicate no palaeolatitudinal offset for the Peninsular Ranges terrane, *J. geophys. Res.,* **103**, 27 169–27 192.

Tan, X., 2001. Correcting the bias toward shallow palaeomagnetic inclinations in haematite-bearing sedimentary rocks: Theory, experiments, and applications, *PhD dissertation,* Lehigh University, Bethlehem, PA.

Tan, X. & Kodama, K.P., 2002. Magnetic anisotropy and palaeomagnetic inclination shallowing in red beds: Evidence from the Mississippian Mauch Chunk Formation, Pennsylvania, *J. geophys. Res.,* in press.

Tan, X., Kodama, K.P. & Fang, D., 2002a. Laboratory depositional and compaction-caused inclination errors carried by haematite and their implications in identifying inclination error of natural remanence in red beds, *Geophys. J. Int.* **151,** 475–486

Tan, X., Kodama, K.P., Chen, H., Fang, D., Sun, D. & Li, Y., 2002b. Palaeomagnetism and magnetic anisotropy of Cretaceous red beds from the Tarim basin, northwest China: Evidence for a rock magnetic cause of anomalously shallow palaeomagnetic inclinations from central Asia, *J. geophys. Res.,* in press.

Tarling, D. & Hrouda, F., 1993. *The Magnetic Anisotropy of Rocks,* Chapman and Hall, London.

Tauxe, L. & Kent, D.V., 1984. Properties of a detrital remanence carried by haematite from study of modern river deposits and laboratory redeposition experiments, *Geophys. J. R. astr. Soc.,* **77**, 543–561.

Uyeda, S., Fuller, M.D., Belshe, J.C. & Girdler, R.W., 1963. Anisotropy of magnetic susceptibility of rocks and minerals, *J. geophys. Res.,* **68**, 279–291.

van der Pluijm, B.A., 1987. Grain scale deformation and the fold test: evaluation of synfolding remagnetization, *Geophys. Res. Lett.,* **14**, 155–157.

van der Pluijm, B.A., Van der Voo, R., Potts, S.S. & Stamatakos, J., 1993. Early Silurian palaeolatitude for Central Newfoundland from palaeomagnetism of the Wigwam Formation: discussion, *Can. J. Earth Sci.,* **30**, 644–645.

Verosub, K.L., 1977. Depositional and post-depositional processes in the magnetization of sediments, *Rev. Geophys. Space Phys.,* **15**, 129–143.

APPENDIX A: DERIVATION OF INCLINATION CORRECTION USING THE TRUNCATED FISHER DISTRIBUTION FUNCTION

Hrouda (1980) adopted a truncated Fisher (1953) distribution function to describe the frequency density of the *c*-axis distribution of haematite particles, and to derive the relationship between bulk sample and individual particle anisotropies. We will use this distribution function to derive the inclination correction expressions.

Based on Hrouda (1980), the frequency density of haematite particles with their *c*-axis distributed in the direction defined by the polar angle θ (Fig. 1) is

$$f = \frac{k}{2\pi(\mathrm{e}^k - 1)}\mathrm{e}^{k\cos\theta} \tag{A1}$$

where k is a measure of concentration of the *c*-axis distribution. This function can also be used to describe the easy-axis distribution of prolate magnetite particles, but with some modifications of the orientation of the principal axes of the bulk sample anisotropy, i.e. the maximum axis will align in the *Z*-axis direction (Fig. 1).

For haematite-bearing samples, the principal axes of the bulk sample anisotropy can be described by

$$\begin{aligned} X &= \int_0^{2\pi}\int_0^{\pi/2} T_{11} f \sin\theta \, d\theta \, d\psi, \\ Y &= \int_0^{2\pi}\int_0^{\pi/2} T_{22} f \sin\theta \, d\theta \, d\psi, \\ Z &= \int_0^{2\pi}\int_0^{\pi/2} T_{33} f \sin\theta \, d\theta \, d\psi. \end{aligned} \tag{A2}$$

The results of the integration in (A2) are

$$X = Y = \frac{L+S}{2} + \frac{L-S}{2}F(k),$$
$$Z = S - (L-S)F(k), \tag{A3}$$
$$F(k) = \frac{k}{e^k - 1}\left[\frac{2}{k^3} - e^k\left(\frac{1}{k} - \frac{2}{k^2} + \frac{2}{k^3}\right)\right].$$

Eq. (A3) is consistent with Hrouda (1980) eq. (5). The normalized principal axes are

$$X_0 = Y_0 = \frac{(L+S) + (L-S)F(k)}{2(L+2S)},$$
$$Z_0 = \frac{S - (L-S)F(k)}{L+2S}. \tag{A4}$$

Inserting the individual particle anisotropy factor, $a = S/L$ into eq. (A4), we have

$$X_0 = Y_0 = \frac{(1+a) + (1-a)F(k)}{2(1+2a)},$$
$$Z_0 = \frac{a - (1-a)F(k)}{1+2a}. \tag{A5}$$

By arranging eq. (A5) for $F(k)$, we have

$$F(k) = \frac{(1+a) - 2(1+2a)X_0}{a-1},$$
$$F(k) = \frac{(1+2a)Z_0 - a}{a-1}. \tag{A6}$$

Assuming an infinite a factor for the intrinsic remanence of the particle, we have the NRM tensor:

$$k_{\mathrm{NRM}} = \begin{bmatrix} [1-F(k)]/4 & 0 & 0 \\ 0 & [1-F(k)]/4 & 0 \\ 0 & 0 & [1+F(k)]/2 \end{bmatrix}. \tag{A7}$$

From eq. (16), we have

$$\tan(I_0) = \frac{1-F(k)}{2+2F(k)}\tan(I_{\mathrm{m}}). \tag{A8}$$

Inserting eq. (A6) using either AMS or ARS parameters into eq. (A8), we then have the inclination correction for haematite-bearing samples:

$$\tan(I_0) = \frac{(2a+1)X_0 - 1}{(2a+1)Z_0 - 1}\tan(I_{\mathrm{m}}). \tag{A9}$$

By writing eq. (A6) for ARS and AMS parameters, respectively, and equating them, we have

$$R_i = \frac{(1+2a_\chi)(a_\gamma - 1)}{(1+2a_\gamma)(a_\chi - 1)}\chi_i + \frac{a_\chi - a_\gamma}{(1+2a_\gamma)(a_\chi - 1)}. \tag{A10}$$

Note that eqs (A9) and (A10) are exactly the same as eqs (20) and (22). This may imply that the linear relationship between the normalized principal axes of remanence anisotropy and magnetic susceptibility anisotropy, and the inclination correction are probably independent from detailed OD models.

For magnetite-bearing samples, since the easy-axis distribution of the prolate magnetite particles is around the Z-axis, the maximum principal axis (X_0) of the bulk sample is along the Z-axis direction, while the intermediate and minimum axes (Y_0 and Z_0) (which are equal) are within the XY plane. From (A4), we have

$$Y_0 = Z_0 = \frac{(L+S) + (L-S)F(k)}{2(L+2S)},$$
$$X_0 = \frac{S - (L-S)F(k)}{L+2S}. \tag{A11}$$

By inserting $a = L/S$ into eq. (A11), we have

$$Y_0 = Z_0 = \frac{(1+a) + (a-1)F(k)}{2(a+2)},$$
$$X_0 = \frac{1 - (a-1)F(k)}{a+2}. \tag{A12}$$

Similarly, it can be shown that the linear relationship between the normalized principal axes of ARS and AMS, and the inclination correction for magnetite-bearing samples derived using the truncated Fisher distribution function are exactly the same as eqs (21) and (18), respectively.